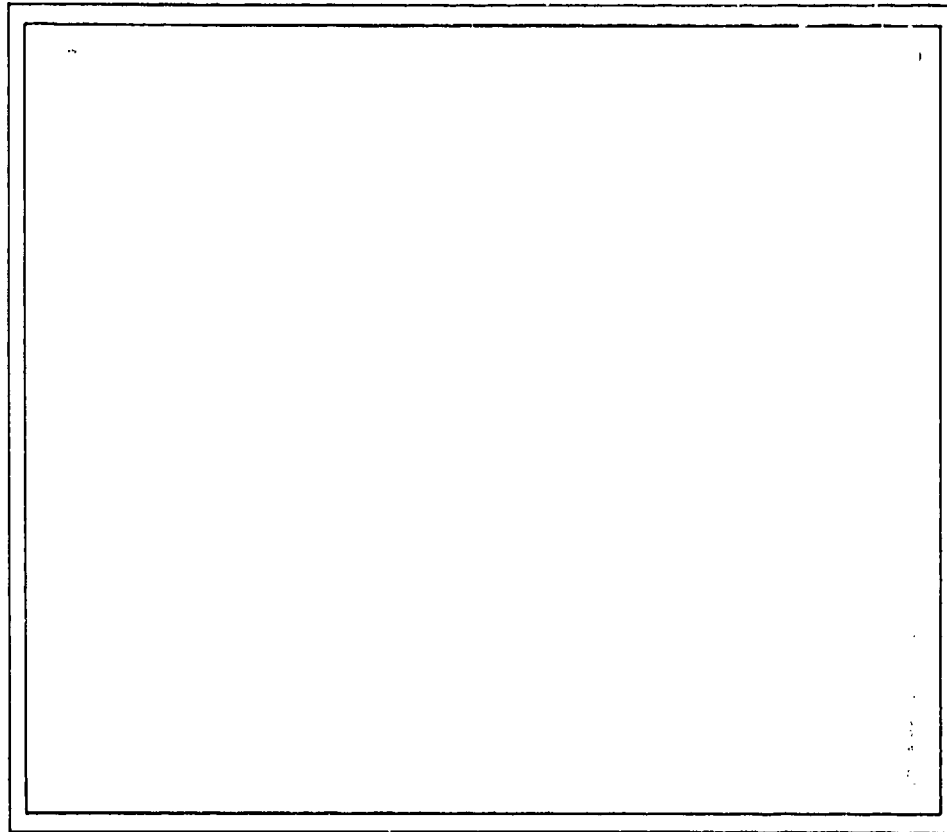


ADA043455

12



PRINCETON UNIVERSITY

Department of Civil Engineering X



D D C
DISTRIBUTION UNLIMITED
AUG 29 1977
B

DISTRIBUTION UNLIMITED	
Approved for public release; Distribution Unlimited	

FILE COPY

STRUCTURES AND MECHANICS

(7) Technical Rept. No. 46
Civil Engng. Res. Rep. No. 77-SM-10 7IR-46

(6) LINE CRACK SUBJECT TO SHEAR.

by

(10) A. Cemal/Eringen

Research Sponsored by the
Office of Naval Research

(15) under
Contract N00014-76-C-0240
Modification No. P00002

ACCESSION for	
NTIS	White Section <input checked="" type="checkbox"/>
DDC	Buff Section <input type="checkbox"/>
UNANNOUNCED	<input type="checkbox"/>
JUSTIFICATION <i>SAE 1472-fm. Fy.b</i>	
BY	
DISTRIBUTION/AVAILABILITY CODES	
DISL. AVAIL. and/or SPECIAL	
A	

(12) DDC
(10) July 1977

D D C
DEPARTMENT OF DEFENSE
DEFENSE DOCUMENTATION CENTER
REPRODUCTION
MADE PURSUANT TO
THE ECONOMIC SECURITY ACT
B

Approved for Public Release; Distribution Unlimited

40127d

1B

LINE CRACK SUBJECT TO SHEAR¹

A. Cemal Eringen

Princeton University
Princeton, NJ 08540

ABSTRACT

Field equations of nonlocal elasticity are solved to determine the state of stress in the neighborhood of a line crack in an elastic plate subject to a uniform shear at the surface of the crack tip. A fracture criterion based on the maximum shear stress gives the critical value of the applied shear for which the crack becomes unstable. Cohesive stress necessary to break the atomic bonds is calculated for brittle materials.

1. INTRODUCTION

In several previous papers, [1] - [3], we discussed the state of stress near the tip of a sharp line crack in an elastic plate subject to a uniform tension perpendicular to the line of the crack at infinity. The solution of this problem was obtained within the framework of the non-local elasticity theory. The resulting solution did not contain the stress singularity present in the classical elasticity solution and therefore a natural fracture criterion based on the usual maximum stress hypothesis could be established. This most interesting outcome could be used to calculate the cohesive stress in various materials.

¹The present work was supported by the Office of Naval Research

The present paper deals with the problem of a line crack in an elastic plate where the crack is subject to a uniform shear load. We employ the field equations of nonlocal elasticity theory to formulate and solve this problem. Gratifyingly the resulting solution does not contain the stress singularity at the crack tip and therefore a fracture criterion based on the maximum shear stress hypothesis can be used to obtain the critical value of the applied shear for which the line crack begins to become unstable. If the concept of the surface energy is used it is possible to calculate the cohesive stress holding the atomic bonds together. For steel (with no dislocations) we give an estimate for the cohesive stress. In section 2 we give a resumé of basic equations of the linear nonlocal elasticity theory. In section 3 the boundary value problem is formulated and the general solution is obtained. In section 4 the solution is given for the dual integral equations completing the solution of the problem of line crack subject to a shear load. Calculations for the shear stress are carried out on a computer and results are discussed in section 5.

2. BASIC EQUATIONS OF NONLOCAL ELASTICITY

The basic equations of linear, homogeneous, isotropic, nonlocal elastic solids, with vanishing body and inertia forces, are (cf. [4, 5])

$$(2.1) \quad t_{kl,k} = 0$$

$$(2.2) \quad t_{kl} = \int_V [\lambda'(|x'-x|)e_{rr}(x')\delta_{kl} + 2\mu'(|x'-x|)e_{kl}(x')]dv(x')$$

$$(2.3) \quad e_{kl} = \frac{1}{2} (u_{k,l} + u_{l,k})$$

where the only difference from classical elasticity is in the stress constitutive equations (2.2) which states that the stress $\tau_{kl}(x)$, at a point x , depends on strains $e_{kl}(x')$, at all points of the body. For homogeneous and isotropic solids the nonlocal elastic moduli $\lambda'(|x'-x|)$ and $\mu'(|x'-x|)$ are functions of the distance between the variable point x' and the fixed point x at which the stress is to be evaluated. The integral in (2.2) is over the volume V of the body enclosed within the surface ∂V .

Throughout this paper we employ cartesian coordinates x_k with the usual convention that a free index takes the values (1, 2, 3) and repeated indices are summed over the range (1, 2, 3). Indices following a comma represent partial differentiation, e.g.

$$u_{k,\ell} \equiv \frac{\partial u_k}{\partial x_\ell}$$

In our previous work [4, 6, 7] we have obtained the forms of $\lambda'(|x'-x|)$ and $\mu'(|x'-x|)$ for which the dispersion curves of plane waves coincide within the entire Brillouin zone with those obtained in the Born-Von Kármán theory of lattice dynamics. Accordingly

$$(2.4) \quad (\lambda', \mu') = (\lambda, \mu)\alpha(|x'-x|),$$

$$\alpha(|x'-x|) = \begin{cases} \alpha_0(a - |x'-x|) & |x'-x| \leq a, \\ 0 & |x'-x| > a \end{cases}$$

where a is the lattice parameter, λ and μ are classical Lamé constants, and α_0 is a normalization constant to be determined from

$$(2.5) \quad \int_V \alpha(|\underline{x}' - \underline{x}|) dV(\underline{x}') = 1$$

While this simple and elegant result is useful in many calculations, it is not the only one that approximates the dispersion curves of lattice dynamics. In fact a very useful one is

$$(2.6) \quad \alpha(|\underline{x}' - \underline{x}|) = \alpha_0 \exp[-(\beta/a)^2 (x'_k - x_k)(x'_k - x_k)]$$

where β is a constant. For the two-dimensional case (2.6) has the specific form

$$(2.7) \quad \alpha(|\underline{x}' - \underline{x}|) = \frac{1}{\pi} (\beta/a)^2 \exp[-(\beta/a)^2 [(x'_{11} - x_{11})^2 + (x'_{12} - x_{12})^2]]$$

Employing (2.4), in (2.2) we write

$$(2.8) \quad t_{kl} = \int_V \alpha(|\underline{x}' - \underline{x}|) \sigma_{kl}(\underline{x}') dV(\underline{x}')$$

where

$$(2.9) \quad \begin{aligned} \sigma_{kl}(\underline{x}') &= \lambda e_{rr}(\underline{x}') \delta_{kl} + 2\mu e_{kl}(\underline{x}') \\ &= \lambda u_{r,r}(\underline{x}') \delta_{kl} + \mu [u_{k,l}(\underline{x}') + u_{l,k}(\underline{x}')] \end{aligned}$$

is the classical Hooke's law. Substituting (2.8) into (2.1) and using the Green-Gauss theorem we obtain

$$(2.10) \quad \int_V \alpha(|\underline{x}' - \underline{x}|) \sigma_{kl,k}(\underline{x}') dV(\underline{x}') - \oint_{\partial V} \alpha(|\underline{x}' - \underline{x}|) \sigma_{kl}(\underline{x}') da_k(\underline{x}') = 0$$

Here the surface integral may be dropped if the only surface of the body is at infinity.

3. CRACK UNDER SHEAR

Consider a plate in $(x_1 \leq x, x_2 \leq y)$ - plane weakened by a line crack of length 2ℓ along the x -axis. The plate is subjected to a constant shear stress τ_0 along the surfaces of the crack, Fig. 1. For the plane strain problem (2.10) takes the form

$$(3.1) \quad \int_R \alpha(|x'-x|) \sigma_{k\ell,k}(x',y') dx' dy' - \int_{-\ell}^{\ell} \alpha(|x'-x|) [\sigma_{2\ell}(x',0)] dx' = 0$$

where the integral with a slash is over the two-dimensional infinite space excluding the crack line ($|x| < \ell, y=0$). A bold-face bracket indicates a jump at the crack line.

When an incision is made in an undeformed body, the body will in general be deformed and stressed because of the long-range interatomic attractions. Thus if we are to treat the problem of a plate with crack, undeformed and unstressed in the natural state, we must consider that after an incision is made the crack is not opened, i.e. the boundary conditions are to be applied to the plate in the natural state.

Under the applied uniform shear load on the unopened surfaces of the crack the displacement field possess the following symmetry regulations

$$(3.2) \quad u(x,-y) = -u(x,y), \quad v(x,-y) = v(x,y)$$

Employing this in (2.9) we see that

$$(3.3) \quad [\bar{\sigma}_{2\ell}(x,0)] = 0 \quad , \quad |x| > \ell$$

Hence the limits $(-\ell, \ell)$ in the second integral of (3.1) may be replaced by $(-\infty, \infty)$.

The Fourier transform of (3.1) with respect to x' gives

$$(3.4) \quad \int_{-\infty}^{\infty} \bar{a}(\xi, |y'-y|) [-i\xi \bar{\sigma}_{1\ell}(\xi, y') + \frac{d}{dy'} \bar{\sigma}_{2\ell}(\xi, y')] dy' \\ -\bar{a}(\xi, |y|) [\bar{\sigma}_{2\ell}(\xi, 0)] = 0$$

where a superposed bar indicates the Fourier transform, e.g.,

$$\bar{f}(\xi, y) = (2\pi)^{\frac{1}{2}} \int_{-\infty}^{\infty} f(x, y) \exp(i\xi x) dx$$

If we take the Fourier transform of (3.4) with respect to y , and solve for the factor of \bar{a} in the integrand of (3.4), upon inversion we obtain

$$-i\xi \bar{\sigma}_{1\ell}(\xi, y) + \frac{d}{dy} \bar{\sigma}_{2\ell}(\xi, y) = (2\pi)^{-\frac{1}{2}} [\bar{\sigma}_{2\ell}(x, 0)] \int_{-\infty}^{\infty} \exp(-iny) dn$$

since the left hand side is defined for all y except $y=0$. Thus we obtain

$$(3.5) \quad -i\xi \bar{\sigma}_{1\ell} + \frac{d\bar{\sigma}_{2\ell}}{dy} = 0 \quad , \quad \ell = 1, 2$$

Substituting this into (3.4) we have

$$(3.6) \quad [\sigma_{2\ell}(x,0)] = 0, \quad \ell = 1, 2$$

Hence we have shown that the general solution of (3.4) is the same as that of the system (3.5) and (3.6).

The jump condition (3.6) for $|x|>\ell$ is satisfied identically. For $|x|<\ell$ we also have $[\sigma_{21}(x,0)] = 0$, on account of (3.2). Since $\sigma_{22}(x,-y) = -\sigma_{22}(x,y)$ we also see that $t_{22}(x,0) = 0$ for $|x|<\ell$. Thus the normal stress condition on the crack surface is satisfied identically. Considering also the continuity requirement of the displacement field satisfying (3.3) we find that the boundary conditions at $x=0$ are:

$$(3.7) \quad \begin{aligned} \sigma_{yy}(x,0) &= 0, & t_{yx}(x,0) &= \tau_0, & |x|<\ell \\ \sigma_{yy}(x,0) &= 0, & u(x,0) &= 0, & |x|>\ell \end{aligned}$$

In addition we must have

$$(3.8) \quad u = v = 0, \quad \text{as } y \rightarrow \infty$$

Consequently we must obtain the solution of (3.5) subject to (3.7) and (3.8).¹

¹Even though some authors feel that $v(x,0)=0$, $|x|>\ell$ should also be satisfied for this (so-called Mode II) problem (cf. [8]), the results based on the boundary conditions (3.7) and (3.8) are accepted by workers on the theory of fracture. The physical reasoning indicates that constant shear load if not balanced by an opposing couple, should give a rotation to the whole body so that $v(x,0)=0$ for $|x|>\ell$ appears to be in contradiction with the expected displacement field.

Equations (3.5) are none other than the Fourier transforms of the Navier's equations in two dimensions, namely

$$\begin{aligned} \mu \bar{u}_{yy} - (\lambda + 2\mu) \xi^2 \bar{u} - i\xi(\lambda + \mu) \bar{v}_y &= 0, \\ (3.9) \quad -i\xi(\lambda + \mu) \bar{u}_y + (\lambda + 2\mu) \bar{v}_{yy} - \xi^2 \mu \bar{v} &= 0 \end{aligned}$$

The general solution of this set (for $y > 0$), satisfying (3.8) is.

$$\begin{aligned} u &= -(2\pi)^{-1/2} \int_{-\infty}^{\infty} \xi^{-1} [|\xi|A(\xi) + (|\xi|y - \frac{\lambda+3\mu}{\lambda+\mu})B(\xi)] \exp(-|\xi|y - i\xi x) d\xi, \\ (3.10) \quad v &= (2\pi)^{-1/2} \int_{-\infty}^{\infty} i[A(\xi) + yB(\xi)] \exp(-|\xi|y - i\xi x) d\xi \end{aligned}$$

where $A(\xi)$ and $B(\xi)$ are to be determined from the boundary conditions (3.7). Using (2.9) we calculate

$$(3.11) \quad \bar{\sigma}_{yy}(\xi, y) = 2\mu i[-|\xi|A(\xi) + (\frac{\mu}{\lambda+\mu} - |\xi|y)B(\xi)] \exp(-|\xi|y)$$

According to (3.7)₁ and (3.7)₃, this must vanish at $y=0$. Hence

$$(3.12) \quad B(\xi) = \frac{\lambda+\mu}{\mu} |\xi| A(\xi)$$

Noting that $A(-\xi) = A(\xi)$, on account of symmetry $u(x, y) = u(-x, y)$, the displacement field may be put into the form

$$\begin{aligned} u(x, y) &= (\frac{2}{\pi})^{1/2} \frac{\lambda+\mu}{\mu} \int_0^{\infty} A(\xi) \left(\frac{\lambda+2\mu}{\lambda+\mu} - \xi y \right) e^{-\xi y} \cos(\xi x) d\xi, \\ (3.13) \quad v(x, y) &= (\frac{2}{\pi})^{1/2} \frac{\lambda+\mu}{\mu} \int_0^{\infty} A(\xi) \left(\frac{\mu}{\lambda+\mu} + \xi y \right) e^{-\xi y} \sin(\xi x) d\xi \end{aligned}$$

For the η_{kl} , through (2.9) and (3.12) we obtain ($y > 0$)

$$(3.14) \quad \begin{aligned} \sigma_{xx}(x, y) &= -\sigma_{xx}(x, -y) = -2(2/\pi)^{1/2}(\lambda+\mu) \int_0^\infty A(\xi)(2\xi - \xi^2 y) e^{-\xi y} \sin(\xi x) d\xi, \\ \sigma_{yy}(x, y) &= -\sigma_{yy}(x, -y) = -2(2/\pi)^{1/2}(\lambda+\mu) \int_0^\infty A(\xi) \xi^2 y e^{-\xi y} \sin(\xi x) d\xi, \\ \sigma_{yx}(x, y) &= \sigma_{xy}(x, -y) = -2(2/\pi)^{1/2}(\lambda+\mu) \int_0^\infty A(\xi) \xi(1-\xi y) e^{-\xi y} \cos(\xi x) d\xi \end{aligned}$$

The stress field according to (2.8), is then given by

$$(3.15) \quad \begin{aligned} t_{xx}(x, y) &= \int_0^\infty dy' \int_{-\infty}^\infty \sigma_{xx}(x', y') [\alpha(|x'-x|, |y'-y|) - \alpha(|x'-x|, |y'+y|)] dx' \\ t_{yy}(x, y) &= \int_0^\infty dy' \int_{-\infty}^\infty \sigma_{yy}(x', y') [\alpha(|x'-x|, |y'-y|) - \alpha(|x'-x|, |y'+y|)] dx' \\ t_{yx}(x, y) &= \int_0^\infty dy' \int_{-\infty}^\infty \sigma_{yx}(x', y') [\alpha(|x'-x|, |y'-y|) + \alpha(|x'-x|, |y'+y|)] dx' \end{aligned}$$

Substituting for α from (2.7), the integrations may be performed with respect to x' and y' by noting the integrals (cf., [9]).

$$(3.16) \quad \begin{aligned} I_1 &= \int_{-\infty}^\infty \exp(-px'^2) \left\{ \begin{array}{l} \sin \xi(x+x') \\ \cos \xi(x+x') \end{array} \right\} dx' = (\pi/p)^{1/2} \exp(-\xi^2/4p) \left\{ \begin{array}{l} \sin \xi x \\ \cos \xi x \end{array} \right\} \\ I_2 &= \int_0^\infty \exp(-py'^2 - \gamma y') dy' = \frac{1}{2} (\pi/p)^{1/2} \exp(\gamma^2/4p) [1 - \Phi(\gamma/2\sqrt{p})], \\ I_3 &= \int_0^\infty y' \exp(-py'^2 - \gamma y') dy' = \frac{1}{2p} - \frac{\gamma}{4p} \left(\frac{\pi}{p} \right)^{1/2} \exp(\gamma^2/4p) [1 - \Phi(\gamma/2\sqrt{p})], \end{aligned}$$

Hence,

$$\begin{aligned}
 t_{xx} &= -(2/\pi)^{\frac{1}{2}}(\lambda+\mu) \int_0^\infty A(\xi) \sin(\xi x) \{ e^{-\xi y} [2\xi + (\xi^2/2p)(\xi - 2py)] \\
 &\quad \cdot [1 - \Phi(\frac{\xi - 2py}{2\sqrt{p}})] - e^{\xi y} [2\xi + (\xi^2/2p)(\xi + 2py)] [1 - \Phi(\frac{\xi + 2py}{2\sqrt{p}})] \} d\xi, \\
 t_{yy} &= (2/\pi)^{\frac{1}{2}}(\lambda+\mu) \int_0^\infty \xi^2 A(\xi) \sin(\xi x) \{ e^{-\xi y} \frac{\xi - 2py}{2p} [1 - \Phi(\frac{\xi - 2py}{2\sqrt{p}})] \\
 &\quad - e^{\xi y} \frac{\xi + 2py}{2p} [1 - \Phi(\frac{\xi + 2py}{2\sqrt{p}})] \} d\xi, \\
 t_{yx} &= -(2/\pi)^{\frac{1}{2}}(\lambda+\mu) \int_0^\infty A(\xi) \xi \cos(\xi x) \{ e^{-\xi y} [1 + (\xi/2p)(\xi - 2py)] \\
 &\quad \cdot [1 - \Phi(\frac{\xi - 2py}{2\sqrt{p}})] + e^{\xi y} [1 + (\xi/2p)(\xi + 2py)] [1 - \Phi(\frac{\xi + 2py}{2\sqrt{p}})] \\
 &\quad - 2\xi(\pi p)^{-\frac{1}{2}} \exp[-py^2 - (\xi^2/4p)] \} d\xi
 \end{aligned} \tag{3.17}$$

where $p = (\beta/a)^2$, and $\Phi(z)$ is the error function defined by

$$\Phi(z) = 2\pi^{-\frac{1}{2}} \int_0^z \exp(-t^2) dt$$

The remaining two boundary conditions $(3.7)_2$ and $(3.7)_4$ may now be expressed as

$$\begin{aligned}
 (3.18) \quad \int_0^\infty \zeta^{\frac{1}{2}} C(\zeta) K(\zeta, p) \cos(\zeta z) d\zeta &= -(\pi/2)^{\frac{1}{2}} T_0, \quad 0 < z < 1 \\
 \int_0^\infty \zeta^{-\frac{1}{2}} C(\zeta) \cos(\zeta z) d\zeta &= 0, \quad z > 1
 \end{aligned}$$

where we have introduced

$$x/\ell \equiv z, \quad \xi \ell \equiv \zeta, \quad A(\xi) \equiv \zeta^{-\frac{1}{2}} C(\zeta),$$

$$(3.19) \quad K(\zeta, p) \equiv [1 + (\zeta^2/2p\ell^2)][1 - \Phi(\zeta/2\ell\sqrt{p})] - (\zeta/\ell\sqrt{\pi p}) \exp(-\zeta^2/4p\ell^2),$$

$$T_0 \equiv \tau_0 \ell^2 / 2(\lambda + \mu), \quad p \equiv (\beta/a)^2$$

To determine the unknown function $A(\xi)$ we must solve the dual integral equations (3.18) for $C(\zeta)$.

4. THE SOLUTION OF DUAL INTEGRAL EQUATIONS

By introducing

$$\cos(\zeta z) = (\pi \zeta z / 2)^{\frac{1}{2}} J_{-\frac{1}{2}}(\zeta z)$$

where $J_v(z)$ is the Bessel's function of order v , we write the system

(3.18) in the form

$$(4.1) \quad \int_0^\infty \zeta C(\zeta) [1 + k(\varepsilon \zeta)] J_{-\frac{1}{2}}(\zeta z) d\zeta = -T_0 z^{-\frac{1}{2}}, \quad 0 < z < 1$$

$$\int_0^\infty C(\zeta) J_{-\frac{1}{2}}(\zeta z) d\zeta = 0, \quad z > 1$$

The kernel function $k(\varepsilon \zeta)$ is given by

$$(4.2) \quad k(\varepsilon \zeta) = K(\zeta, p) - 1 = 2\varepsilon^2 \zeta^2 [1 - \Phi(\varepsilon \zeta)] - \Phi(\varepsilon \zeta) - 2\pi^{-\frac{1}{2}} \varepsilon \zeta \exp(-\varepsilon^2 \zeta^2)$$

where

$$(4.3) \quad \varepsilon \equiv 1/2\ell p^{\frac{1}{2}} = a/2\beta\ell$$

The solution of the dual integral equations (4.1) is not known. However, it is possible to reduce the problem to the solution of a Fredholm equation (see [10] § 4.6).

$$(4.4) \quad h(x) + \int_0^1 h(u)L(x,u)du = -\frac{1}{2}(\pi x)^{\frac{1}{2}}T_0$$

for the function $h(x)$, where

$$(4.5) \quad L(x,u) = (xu)^{\frac{1}{2}} \int_0^\infty tk(\varepsilon t)J_0(xt)J_0(ut)dt$$

Once (4.4) is solved then $C(\zeta)$ is calculated by

$$(4.6) \quad C(\zeta) = (2\zeta)^{\frac{1}{2}} \int_0^1 x^{\frac{1}{2}} J_0(\zeta x)h(x)dx$$

We observe that for $\varepsilon=0$ we have $k=0$, and the dual integral equations (4.1) reduce to those obtained in the classical elasticity. For this case from (4.4) we have $h_0(x) = -T_0(\pi x)^{\frac{1}{2}}/2$, and (4.6) gives the classical result:

$$(4.7) \quad C_0(\zeta) = -(\pi/2)^{\frac{1}{2}} T_0 \zeta^{-\frac{1}{2}} J_1(\zeta)$$

or

$$(4.8) \quad A_0(\xi) = -(\pi/2)^{\frac{1}{2}} T_0 J_1(\xi\ell)/\xi\ell$$

The next iteration of the integral equation (4.4) with the use of $h_0(x)$ gives

$$(4.9) \quad h_1(x) = -(\pi/2)^{\frac{1}{2}} T_0 \zeta^{\frac{1}{2}} [\zeta^{-1} J_1(\zeta) - I(\zeta, \epsilon)]$$

where

$$(4.10) \quad I(\zeta, \epsilon) \equiv \int_0^1 x J_0(\zeta x) \hat{f}(x, \epsilon) dx$$

$$(4.11) \quad = \int_0^\infty \frac{k(\epsilon t) J_1(t)}{\zeta^2 - t^2} [\zeta J_0(t) J_1(\zeta) - t J_0(\zeta) J_1(t)] dt$$

In which \hat{f} is the Hankel transform of $t^{-1} k(\epsilon t) J_1(t)$, i.e.,

$$\hat{f}(x, \epsilon) \equiv \int_0^\infty t f(t, \epsilon) J_1(xt) dt,$$

$$f(t, \epsilon) \equiv t^{-1} k(\epsilon t) J_1(t)$$

If we write

$$x/\epsilon = y, \quad \epsilon \zeta = \eta$$

in (4.10), we will have

$$I(\zeta, \epsilon) = \epsilon^2 \int_0^{1/\epsilon} J_0(\eta y) \hat{f}(\epsilon y, \epsilon) dy$$

But since $\epsilon^2 \hat{f}(\epsilon y, \epsilon)$ is the Hankel transform of $f(\eta/\epsilon, \epsilon)$, we see that

$$\lim_{\epsilon \rightarrow 0} I(\zeta, \epsilon) = \lim_{\epsilon \rightarrow 0} f(\zeta, \epsilon) = \lim_{\epsilon \rightarrow 0} [\zeta^{-1} J_1(\zeta) k(\epsilon \zeta)]$$

Hence (4.10) vanishes as $k(\epsilon\zeta)$ with $\epsilon \rightarrow 0$, i.e.,

$$(4.12) \quad C_1(\zeta) = -(\pi/2)^{\frac{1}{2}} T_0 \zeta^{-\frac{1}{2}} J_0(\zeta) + O(\zeta)$$

Thus for small ϵ the difference between $C_0(\zeta)$ and $C_1(\zeta)$ will be of order ϵ . Since any number of iterations will contribute higher order terms in ϵ , the solution for $C(\zeta)$ will also be in the form (4.12) as $\epsilon \rightarrow 0$.

We observe that in general β is in the neighborhood of 1, [6]. The ratio of the atomic distance to the crack length $a/2l$ is, however, extremely small for even microscopic cracks. Thus ϵ is very small and $k(\epsilon\zeta)$ is in general negligible as compared to unity for all values of $\epsilon\zeta$. As can be seen from Fig. 2, $k(\epsilon\zeta)$ goes uniformly from 0 to -1 as $\epsilon\zeta$ varies between 0 and ∞ . Thus we expect that the solution of (4.1) for $C(\zeta)$ will be almost the same as the classical solution $C_0(\zeta)$ corresponding to $\epsilon=0$. Some differences are of course expected for crack lengths close to atomic distances.

Substituting $A_0(\zeta)$ for $A(\zeta)$ in (3.13) and (3.17), we obtain the displacement and stress fields. It is of interest to calculate the shear stress along the x-axis. This is given by

$$(4.13) \quad t_{yx}/\tau_0 = \int_0^\infty [1+k(\epsilon\zeta)] J_1(\zeta) \cos(\zeta z) d\zeta, \quad z \equiv x/l$$

This integral for $0 < z < 1$ gives $t_{yx}/\tau_0 = 1$ since in this interval the integral converges even for $\epsilon=0$. For $z > 1$ the integral again converges for all $\epsilon > 0$ and it is permissible to ignore $k(\epsilon\zeta)$ as compared to unity. However for $z=1$ this is no longer the case and we cannot ignore $k(\epsilon\zeta)$ as compared to unity. To see this we write t_{yx} at $z=1$ as:

$$t_{yx}(x, \ell) = t_1 + t_2 + t_3$$

where

$$\begin{aligned} t_1 &= \tau_0 \int_0^\infty J_1(n) [1-\Phi(\epsilon n)] \cos n \eta \, dn, \\ t_2 &= 2\tau_0 \int_0^\infty \epsilon^2 n^2 J_1(n) [1-\Phi(\epsilon n)] \cos n \eta \, dn, \\ t_3 &= -2\tau_0 \pi^{-\frac{1}{2}} \int_0^\infty \epsilon n J_1(n) \exp(-\epsilon^2 n^2) \cos n \eta \, dn \end{aligned}$$

Since $1-\Phi(\epsilon n) \geq 0$ and $\tau_0 \geq 0$ it is clear that

$$|t_1| \leq (\tau_0 / \epsilon) \int_0^\infty [1-\Phi(y)] dy = \tau_0 / \pi^{\frac{1}{2}} \epsilon ,$$

$$|t_2| \leq (2\tau_0 / \epsilon) \int_0^\infty y^2 [1-\Phi(y)] dy = 4\tau_0 / 3\pi^{\frac{1}{2}} \epsilon ,$$

$$|t_3| \leq (2\tau_0 / \pi^{\frac{1}{2}} \epsilon) \int_0^\infty \exp(-y^2) dy = \tau_0 / \pi^{\frac{1}{2}} \epsilon$$

Hence

$$|t_{yx}(x, \ell)| \leq \left(\frac{10}{3} \tau_0 \pi^{-\frac{1}{2}} \right) \epsilon^{-1}$$

Thus we see that $t_{yx}(x, \ell)$ has finite value for $\epsilon \neq 0$. In the evaluation of the stress field near $z=1+$, therefore we cannot ignore the function $k(\epsilon \zeta)$ in (4.13).

5. NUMERICAL ANALYSIS AND DISCUSSION

Calculations of the shear stress t_{yx} , given by (4.13) along the crack line, were carried out on computer. The results are plotted for $\epsilon=1/20, 1/50, 1/100$ and $1/200$ in Figures 3 to 6. For a crack length of 20 atomic distance ($\epsilon=1/20$) the results are not very good. However for a crack length of 100 atomic distances (Fig. 5) we can see that the shear stress boundary condition $t_{yx}(x,0)=\tau_0$ for $|x|<\ell$ is satisfied in a strong approximate sense. The relative error is less than 1% o. Hence we conclude that the use of the classical $A_0(\xi)$ given by (4.8) gives satisfactory results for crack lengths greater than 100 atomic distances.

The stress concentration occurs at the crack tip, and it is given by

$$(5.1) \quad t_{yx}(\ell,0)/\tau_0 = c/\sqrt{\epsilon}, \quad \epsilon \equiv \beta a/2\ell$$

where c converges to about -0.30, i.e.

$$(5.2) \quad c \approx -0.30$$

We now make the following significant observations:

- (i) The maximum shear stress occurs at the crack tip, and it is finite (eq. 5.1).
- (ii) The shear stress at the crack tip becomes infinite as the atomic distance $a \rightarrow 0$. This is the classical continuum limit of square root singularity.

(iii) When $t_{yx}(\ell, 0) = t_c$ ($=$ cohesive shear stress), fracture will occur. In this case

$$(5.3) \quad \tau_0^2 \ell = G_c$$

where

$$(5.4) \quad G_c = (\beta a / 2c^2) t_c^2$$

Equation (5.3) is non other than the expression of the Griffith criterion for brittle fracture. Note that we have arrived at this criterion via the maximum shear stress hypothesis. The present criterion of fracture not only unifies the fracture mechanics at the macroscopic and microscopic scales, but also employs the natural concept of bond failure in the atomic scale.

(iv) The cohesive stress t_c may be estimated if one employs the Griffith definition of surface energy γ and writes

$$(5.5) \quad t_c^2 a = K_c \gamma ,$$

where

$$(5.6) \quad K_c = 8c^2 \mu / \pi \beta (1-\nu)$$

Employing the values of γ and the elastic constants for steel

$$\gamma = 1975 \text{ CGS} , \quad \mu = 6.92 \times 10^{11} \text{ CGS}$$

$$\nu = 0.291 , \quad a = 2.48 \text{ A}^0 , \quad \beta = 1.65$$

we find that¹:

$$t_c = 1.04 \times 10^{11} \text{ CGS} , \quad t_c/\mu \approx 0.15$$

This result is in the right range and well accepted by metallurgists based on other considerations. For example Kelly [11] gives

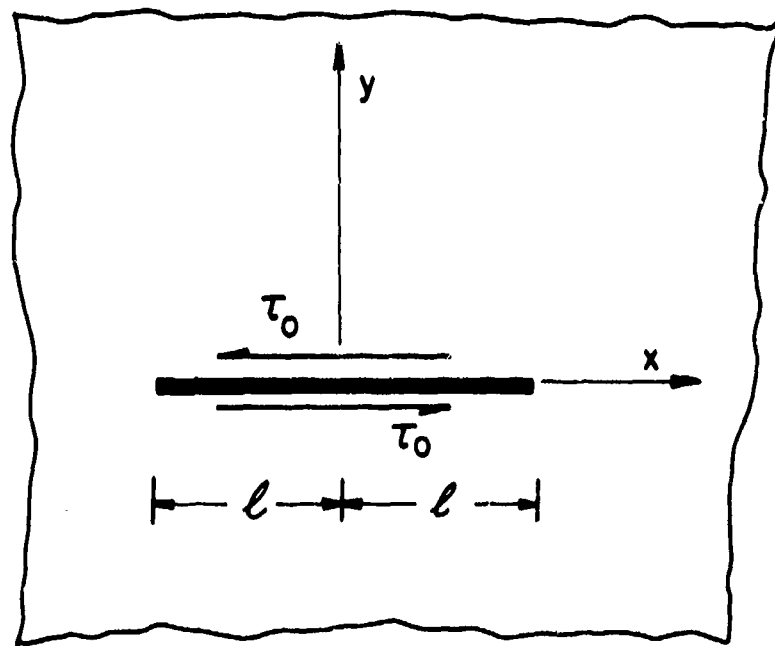
$$t_c \approx 6.0 \times 10^{10} \text{ CGS} \text{ and } t_c/\mu = 0.11.$$

Acknowledgement: The author is indebted to Dr. L. Hajdo for carrying out the computations.

¹The attenuation constant $\beta=1.65$, used in these calculations, makes the Fourier transform of α coincide with the dispersion curve of elastic waves in Born-Von Kármán model of lattice dynamics (cf. [6]).

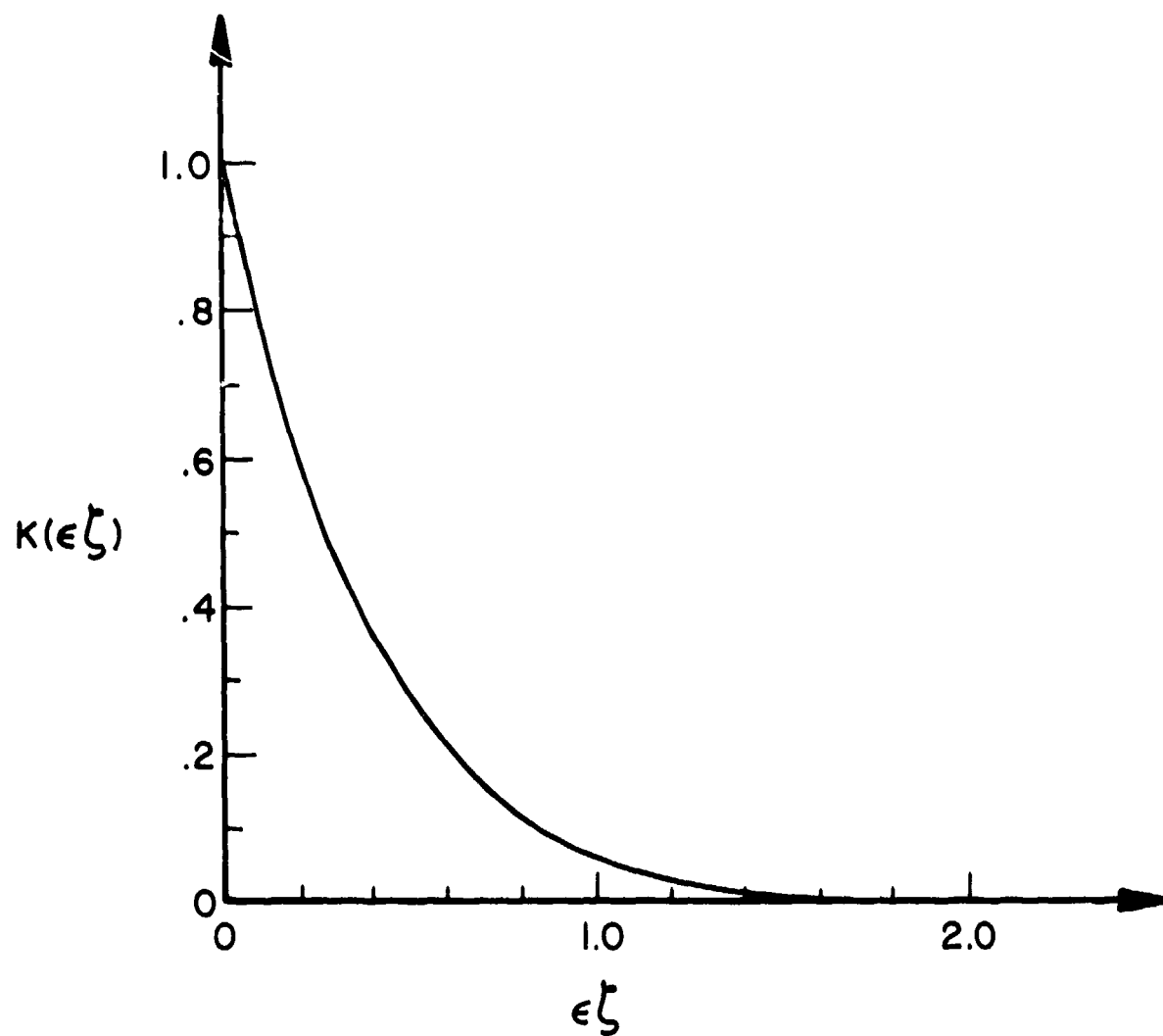
REFERENCES

- [1] A. C. Eringen and B. S. Kim, "Stress Concentration at the Tip of Crack," Mech. Res. Comm. 1, 233-237. 1974.
- [2] A. C. Eringen, "State of Stress in the Neighborhood of a Sharp Crack Tip," Trans. of the twenty-second conf. of Army mathematicians, 1-18, 1977.
- [3] A. C. Eringen, C. G. Speziale and B. S. Kim, "Crack Tip Problem in Nonlocal Elasticity", to appear in J. Mech. and Phys. of Solids.
- [4] A. C. Eringen, "Linear Theory of Nonlocal Elasticity and Dispersion of Plane Waves", Int. J. Engng. Sci. 10, 233-248, 1972.
- [5] A. C. Eringen, Continuum Physics Volume IV Acad. Press, §7, 1976.
- [6] A. C. Eringen, "Continuum Mechanics at the Atomic Scale", to appear in Cryst. Lattice Defects.
- [7] A. C. Eringen, "Nonlocal Elasticity and Waves" Continuum Mechanics Aspects of Geodynamics and Rock Fracture Mechanics, (ed. P. Thoft-Christensen) Dordrecht, Holland, D. Reidel Publishing Co., pp. 81-105.
- [8] I. N. Sneddon and M. Lowengrub, "Crack Problems in the Mathematical Theory of Elasticity", John Wiley & Sons, New York, 1969, pp. 32-37.
- [9] I. S. Gradshteyn and I. W. Rhyzhik, "Tables of Integrals, Series and Products", New York; Acad. Press, 1965, pp. 489, 307, 338.
- [10] I. N. Sneddon, "Mixed Boundary Value Problems in Potential Theory", North Holland Publ. Co., Amsterdam, 1966, pp. 106-108.
- [11] A. Kelly, "Strong Solids", Oxford, 1966, p. 19.



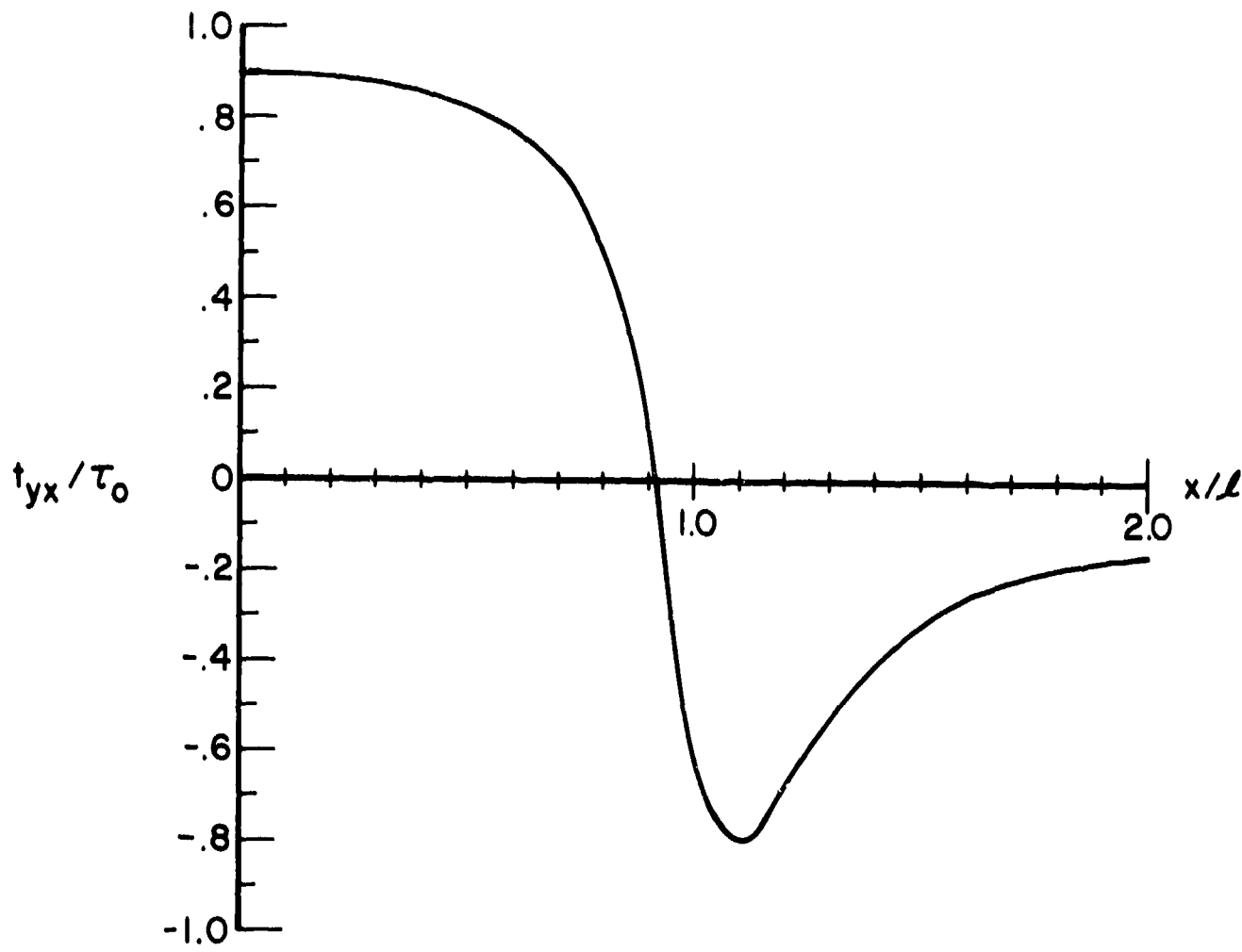
LINE CRACK UNDER SHEAR

FIGURE 1



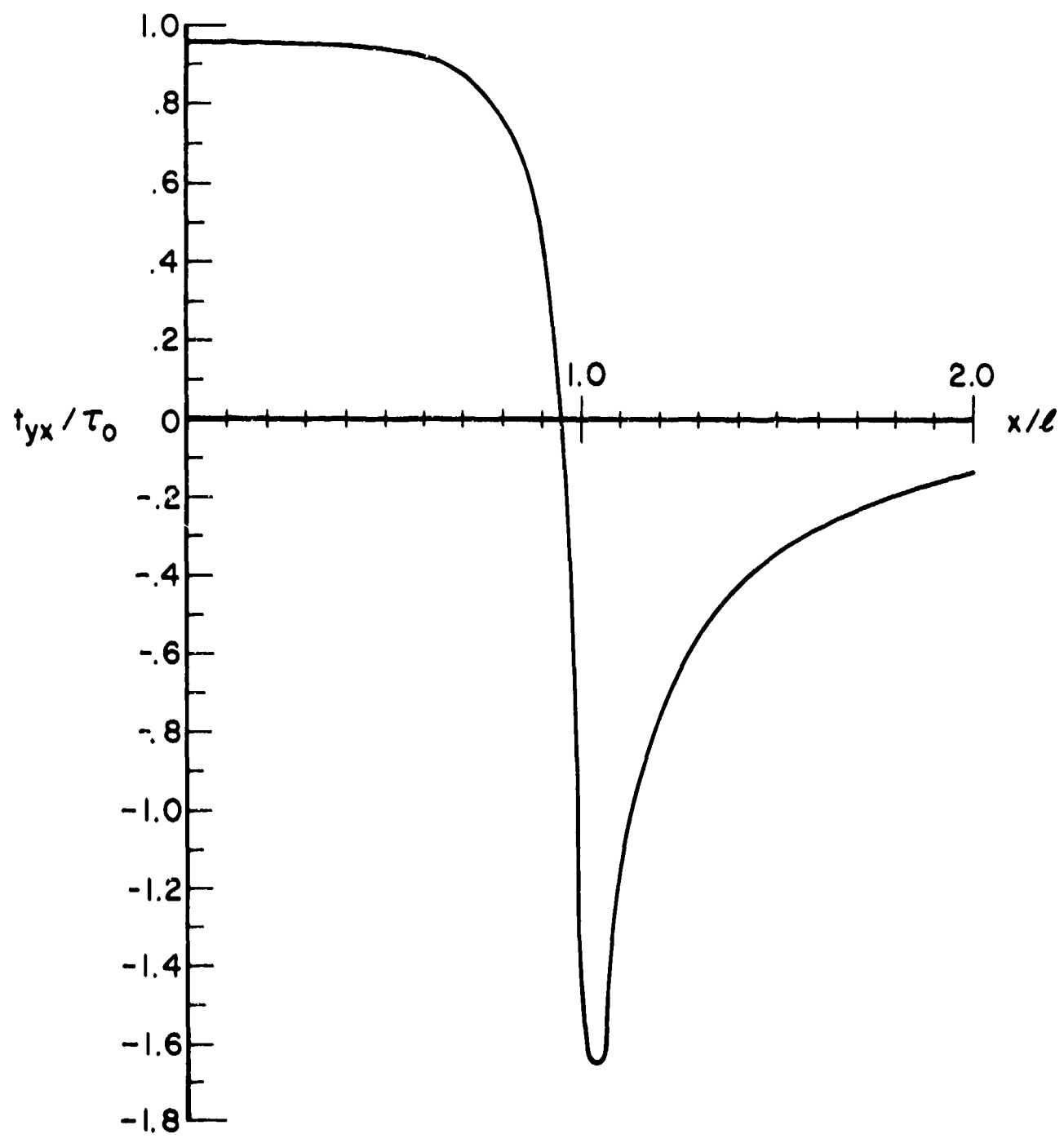
THE BEHAVIOR OF $K(\epsilon \zeta)$ VS $\epsilon \zeta$

FIGURE 2



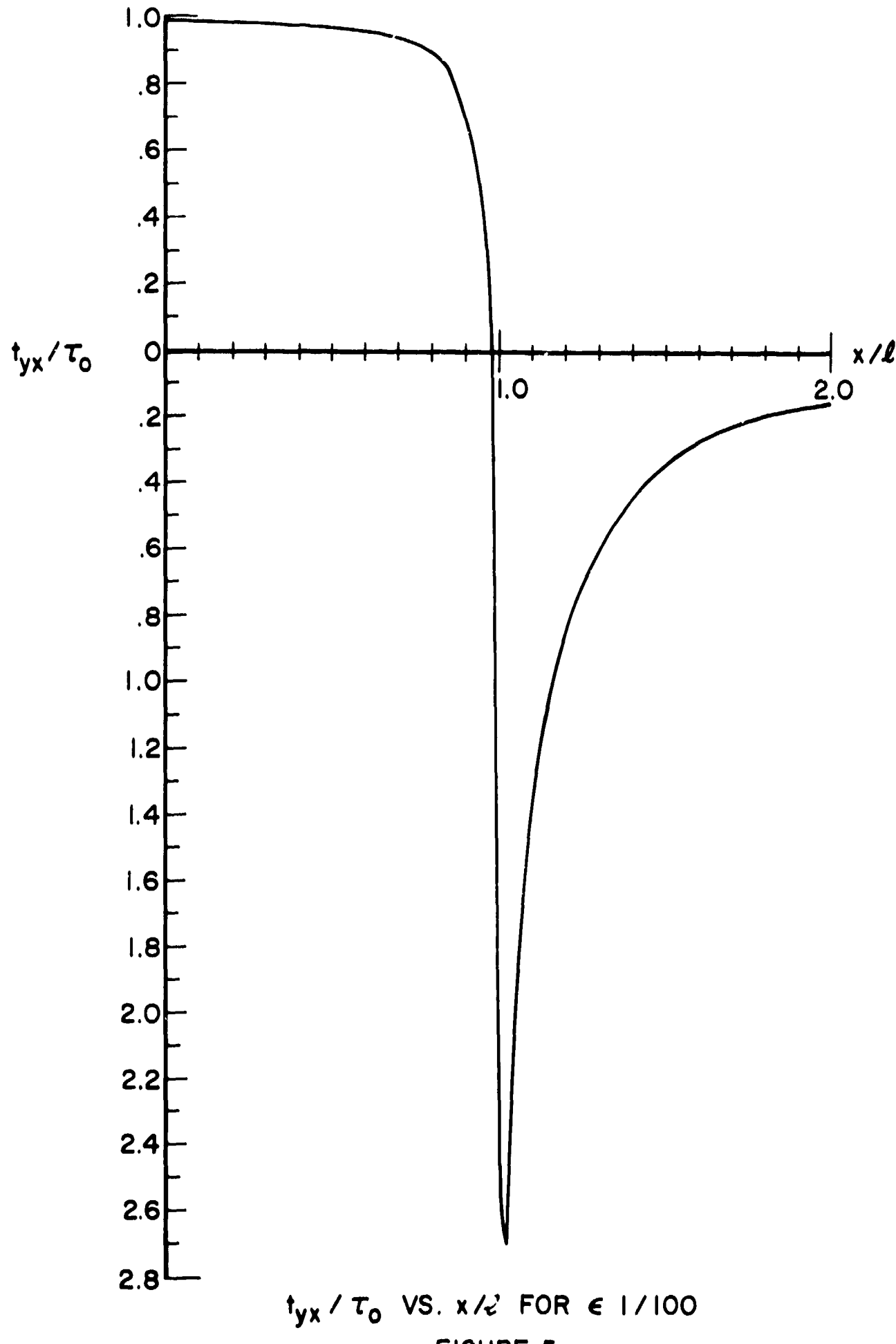
t_{yx}/τ_0 VS. x/ℓ FOR $\epsilon = 1/20$

FIGURE 3



t_{yx}/τ_0 VS. x/ℓ FOR $\epsilon = 1/50$

FIGURE 4



t_{yx} / τ_0 VS. x/l FOR $\epsilon = 1/100$

FIGURE 5

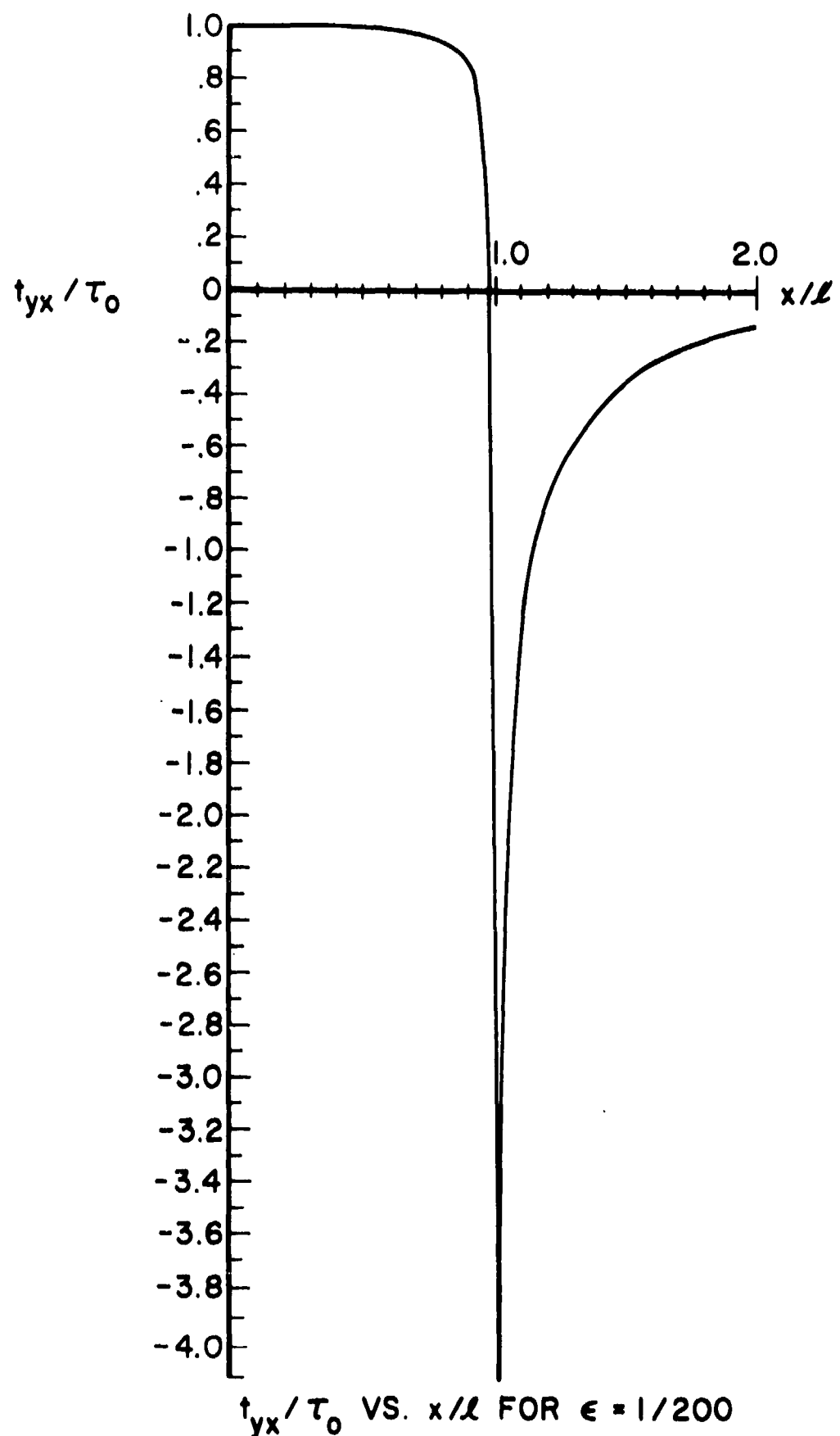


FIGURE 6

SECURITY CLASSIFICATION OF THIS PAGE (When Data Entered)

REPORT DOCUMENTATION PAGE		READ INSTRUCTIONS BEFORE COMPLETING FORM
1. REPORT NUMBER Technical Report 46	2. GOVT ACCESSION NO.	3. RECIPIENT'S CATALOG NUMBER
4. TITLE (and Subtitle) Line Crack Subject to Shear		5. TYPE OF REPORT & PERIOD COVERED Technical Report
		6. PERFORMING ORG. REPORT NUMBER
7. AUTHOR(s) A. Cemal Eringen		8. CONTRACT OR GRANT NUMBER(s) N00014-76-C-0240
9. PERFORMING ORGANIZATION NAME AND ADDRESS Princeton University Princeton, New Jersey 08540		10. PROGRAM ELEMENT, PROJECT, TASK AREA & WORK UNIT NUMBERS P00002
11. CONTROLLING OFFICE NAME AND ADDRESS Office of Naval Research (Code 471) Arlington, VA 22217		12. REPORT DATE July 1977
		13. NUMBER OF PAGES 20
14. MONITORING AGENCY NAME & ADDRESS (if different from Controlling Office)		15. SECURITY CLASS. (of this report) Unclassified
		15a. DECLASSIFICATION/DOWNGRADING SCHEDULE
16. DISTRIBUTION STATEMENT (of this Report) Approved for public release; Distribution Unlimited		
17. DISTRIBUTION STATEMENT (of the abstract entered in Block 20, if different from Report)		
18. SUPPLEMENTARY NOTES		
19. KEY WORDS (Continue on reverse side if necessary and identify by block number) line crack crack under shear nonlocal elasticity theoretical shear stress		
20. ABSTRACT (Continue on reverse side if necessary and identify by block number) Field equations of nonlocal elasticity are solved to determine the state of stress in the neighborhood of a line crack in an elastic plate subject to a uniform shear at the surface of the crack tip. A fracture criterion based on the maximum shear stress gives the critical value of the applied shear for which the crack becomes unstable. Cohesive stress necessary to break the atomic bonds is calculated for brittle materials.		

PART I - GOVERNMENT

Administrative & Liaison Activities

Chief of Naval Research
Department of the Navy
Arlington, Virginia 22217
Attn: Code 474 (2)
471
222

Director
ONR Branch Office
105 Summer Street
Boston, Massachusetts 02210

Director
ONR Branch Office
219 S. Dearborn Street
Chicago, Illinois 60604

Director
Naval Research Laboratory
Attn: Code 2629 (ONRL)
Washington, D.C. 20390 (6)

U.S. Naval Research Laboratory
Attn: Code 2627
Washington, D.C. 20390

Director
ONR - New York Area Office
715 Broadway - 5th Floor
New York, N.Y. 10003

Director
ONR Branch Office
1030 E. Green Street
Pasadena, California 91101

Defense Documentation Center
Cameron Station
Alexandria, Virginia 22314 (12)

Army

Commanding Officer
U.S. Army Research Office Durham
Attn: Mr. J. J. Murray
CRD-AA-IP
Box CM, Duke Station
Durham, North Carolina 27706 2

Commanding Officer
AMXMR-ATL
Attn: Mr. R. Shea
U.S. Army Materials Res. Agency
Watertown, Massachusetts 02172

Watervliet Arsenal
MAGGS Research Center
Watervliet, New York 12189
Attn: Director of Research

Technical Library

Redstone Scientific Info. Center
Chief, Document Section
U.S. Army Missile Command
Redstone Arsenal, Alabama 35809

Army R&D Center
Fort Belvoir, Virginia 22060

Navy

Commanding Officer and Director
Naval Ship Research & Development Center
Bethesda, Maryland 20034
Attn: Code 042 (Tech. Lib. Br.)

17 (Struc. Mech. Lab.)

172

172

174

177

1800 (Appl. Math. Lab.)

5412S (Dr. W.D. Sette)

19 (Dr. M.M. Sevik)

1901 (Dr. M. Strassberg)

1945

196

(Dr. D Feit)

1962

Naval Weapons Laboratory
Dahlgren, Virginia 22448

Naval Research Laboratory
Washington, D.C. 20375

Attn: Code 8400

8410

8430

8440

6300

6390

6380

Undersea Explosion Research Div.
Naval Ship R&D Center
Norfolk Naval Shipyard
Portsmouth, Virginia 23709
Attn: Dr. E. Palmer
Code 780

Naval Ship Research & Development Center
Annapolis Division
Annapolis, Maryland 21402
Attn: Code 2740 - Dr. Y.F. Wang
28 Mr. R.J. Wolfe
281 Mr. R.B. Niederberger
2814 Dr. H. Vanderveldt

Technical Library
Naval Underwater Weapons Center
Pasadena Annex
3202 E. Foothill Blvd.
Pasadena, California 91107

U.S. Naval Weapons Center
China Lake, California 93557
Attn: Code 4062 - Mr. W. Werback
4520 - Mr. Ken Bischel

Commanding Officer
U.S. Naval Civil Engr. Lab.
Code L31
Port Hueneme, California 93041

Technical Director
U.S. Naval Ordnance Laboratory
White Oak
Silver Spring, Maryland 20910

Technical Director
Naval Undersea R&D Center
San Diego, California 92132

Supervisor of Shipbuilding
U.S. Navy
Newport News, Virginia 23607

Technical Director
Mare Island Naval Shipyard
Vallejo, California 94592

U.S. Navy Underwater Sound Ref. Lab.
Office of Naval Research
P.O. Box 8337
Orlando, Florida 32806

Chief of Naval Operations
Dept. of the Navy
Washington, D.C. 20350
Attn: Code Op07T

Strategic Systems Project Office
Department of the Navy
Washington, D.C. 20390
Attn: NSP-001 Chief Scientist

Deep Submergence Systems
Naval Ship Systems Command
Code 39522
Department of the Navy
Washington, D.C. 20360

Engineering Dept.
U.S. Naval Academy
Annapolis, Maryland 21402

Naval Air Systems Command
Dept. of the Navy
Washington, D.C. 20360
Attn: NAVAIR 5302 Aero & Structures
5308 Structures
52031F Materials
604 Tech. Library
320B Structures
Director, Aero Mechanics
Naval Air Development Center
Johnsville
Warminster, Pennsylvania 18974

Technical Director
U.S. Naval Undersea R&D Center
San Diego, California 92132

Engineering Department
U.S. Naval Academy
Annapolis, Maryland 21402

Naval Facilities Engineering Command
Dept. of the Navy
Washington, D.C. 20360
Attn: NAVFAC 03 Research & Development
04 " "
14114 Tech. Library

Naval Sea Systems Command
Dept. of the Navy
Washington, D.C. 20360
Attn: NAVSHIP 03 Res. & Technology
031 Ch. Scientist for R&D
03412 Hydromechanics
037 Ship Silencing Div.
035 Weapons Dynamics

Naval Ship Engineering Center
Prince George's Plaza
Hyattsville, Maryland 20782
Attn: NAVSEC 6100 Ship Sys Engr & Des Dep
6102C Computer-Aided Ship Des
6105G
6110 Ship Concept Design
6120 Hull Div.
6120D Hull Div.
6128 Surface Ship Struct.
6129 Submarine Struct.

Air Force

Commander WADD
Wright-Patterson Air Force Base
Dayton, Ohio 45433
Attn: Code WWRMDD
AFFDL (FDDS)
Structures Division
AFLC (MCEEA)

Chief, Applied Mechanics Group
U.S. Air Force Inst. of Tech.
Wright-Patterson Air Force Base
Dayton, Ohio 45433

Chief, Civil Engineering Branch
WLRC, Research Division
Air Force Weapons Laboratory
Kirtland AFB, New Mexico 87117

Air Force Office of Scientific Research
1400 Wilson Blvd.
Arlington, Virginia 22209
Attn: Mechanics Div.

NASA

Structures Research Division
National Aeronautics & Space Admin.
Langley Research Center
Langley Station
Hampton, Virginia 23365

National Aeronautic & Space Admin.
Associate Administrator for Advanced
Research & Technology
Washington, D.C. 02546

Scientific & Tech. Info. Facility
NASA Representative (S-AK/DL)
P.O. Box 5700
Bethesda, Maryland 20014

Other Government Activities

Commandant
Chief, Testing & Development Div.
U.S. Coast Guard
1300 E. Street, N.W.
Washington, D.C. 20226

Technical Director
Marine Corps Dev. & Educ. Command
Quantico, Virginia 22134

Director
National Bureau of Standards
Washington, D.C. 20234
Attn: Mr. B.L. Wilson, EM 219

Dr. M. Gaus
National Science Foundation
Engineering Division
Washington, D.C. 20550

Science & Tech. Division
Library of Congress
Washington, D.C. 20540

Director
Defense Nuclear Agency
Washington, D.C. 20305
Attn: SPSS

Commander Field Command
Defense Nuclear Agency
Sandia Base
Albuquerque, New Mexico 87115

Director Defense Research & Engrg
Technical Library
Room 3C-128
The Pentagon
Washington, D.C. 20301

Chief, Airframe & Equipment Branch
FS-120
Office of Flight Standards
Federal Aviation Agency
Washington, D.C. 20553

Chief, Research and Development
Maritime Administration
Washington, D.C. 20235

Deputy Chief, Office of Ship Constr.
Maritime Administration
Washington, D.C. 20235
A/Hr. Mr. U. L. Russell

Atomic Energy Commission
Div. of Reactor Devel. & Tech.
Germantown, Maryland 20767

Ship Hull Research Committee
National Research Council
National Academy of Sciences
2101 Constitution Avenue
Washington, D.C. 20418
Attn: Mr. A.R. Lytle

PAK 2 - CONTRACTORS AND OTHER
TECHNICAL COLLABORATORS

Universities

Dr. J. Tinsley Oden
University of Texas at Austin
345 Eng. Science Bldg.
Austin, Texas 78712

Prof. Julius Miklowitz
California Institute of Technology
Div. of Engineering & Applied Sciences
Pasadena, California 91109

Dr. Harold Liebowitz, Dean
School of Engr. & Applied Science
George Washington University
725 - 23rd St., N.W.
Washington, D.C. 20006

Prof. Eli Sternberg
California Institute of Technology
Div. of Engr. & Applied Sciences
Pasadena, California 91109

Prof. Paul M. Naghdif
University of California
Div. of Applied Mechanics
Etcheverry Hall
Berkeley, California 94720

Professor P. S. Symonds
Brown University
Division of Engineering
Providence, R.I. 02912

Prof. A. J. Durelli
The Catholic University of America
Civil/Mechanical Engineering
Washington, D.C. 20017

Prof. R.B. Testa
Columbia University
Dept. of Civil Engineering
S.W. Mudd Bldg.
New York, N.Y. 10027

Prof. H. H. Bleich
Columbia University
Dept. of Civil Engineering
Amsterdam & 120th St.
New York, N.Y. 10027

Prof. F.L. DiMaggio
Columbia University
Dept. of Civil Engineering
616 Mudd Building
New York, N.Y. 10027

Prof. A.M. Freudenthal
George Washington University
School of Engineering &
Applied Science
Washington, D.C. 20006

D. C. Evans
University of Utah
Computer Science Division
Salt Lake City, Wash 84112

Prof. Norman Jones
Massachusetts Inst. of Technology
Dept. of Naval Architecture &
Marine Engrng
Cambridge, Massachusetts 02139

Professor Albert I. King
Biomechanics Research Center
Wayne State University
Detroit, Michigan 48202

Dr. V. R. Hodgson
Wayne State University
School of Medicine
Detroit, Michigan 48202

Dean B. A. Boley
Northwestern University
Technological Institute
2145 Sheridan Road
Evanston, Illinois 60201

Prof. P.G. Hodge, Jr.
University of Minnesota
Dept. of Aerospace Engng & Mechanics
Minneapolis, Minnesota 55455

Dr. D.C. Drucker
University of Illinois
Dean of Engineering
Urbana, Illinois 61801

Prof. N.M. Newmark
University of Illinois
Dept. of Civil Engineering
Urbana, Illinois 61801

Prof. E. Reissner
University of California, San Diego
Dept. of Applied Mechanics
La Jolla, California 92037

Prof. William A. Nash
University of Massachusetts
Dept. of Mechanics & Aerospace Engng.
Amherst, Massachusetts 01002

Library (Code 0384)
U.S. Naval Postgraduate School
Monterey, California 93940

Prof. Arnold Allentuch
Newark College of Engineering
Dept. of Mechanical Engineering
323 High Street
Newark, New Jersey 07102

Dr. George Herrmann
Stanford University
Dept. of Applied Mechanics
Stanford, California 94305

Prof. J. D. Achenbach
Northwestern University
Dept. of Civil Engineering
Evanston, Illinois 60201

Director, Applied Research Lab.
Pennsylvania State University
P. O. Box 30
State College, Pennsylvania 16801

Prof. Eugen J. Skodrzyk
Pennsylvania State University
Applied Research Laboratory
Dept. of Physics - P.O. Box 30
State College, Pennsylvania 16801

Prof. J. Kempner
Polytechnic Institute of Brooklyn
Dept. of Aero. Engrg. & Applied Mech
333 Jay Street
Brooklyn, N.Y. 11201

Prof. J. Klosner
Polytechnic Institute of Brooklyn
Dept. of Aerospace & Appl. Mech.
333 Jay Street
Brooklyn, N.Y. 11201

Prof. R.A. Schapery
Texas A&M University
Dept. of Civil Engineering
College Station, Texas 77840

Prof. W.D. Pilkey
University of Virginia
Dept. of Aerospace Engineering
Charlottesville, Virginia 22903

Dr. H.G. Schaeffer
University of Maryland
Aerospace Engineering Dept.
College Park, Maryland 20742

Prof. K.D. Willmert
Clarkson College of Technology
Dept. of Mechanical Engineering
Potsdam, N.Y. 13676

Dr. J.A. Stricklin
Texas A&M University
Aerospace Engineering Dept.
College Station, Texas 77843

Dr. L.A. Schmit
University of California, LA
School of Engineering & Applied Science
Los Angeles, California 90024

Dr. H.A. Kamel
The University of Arizona
Aerospace & Mech. Engineering Dept.
Tucson, Arizona 85721

Dr. B.S. Berger
University of Maryland
Dept. of Mechanical Engineering
College Park, Maryland 20742

Prof. G. R. Irwin
Dept. of Mechanical Engrg.
University of Maryland
College Park, Maryland 20742

Dr. S.J. Fenves
Carnegie-Mellon University
Dept. of Civil Engineering
Schenley Park
Pittsburgh, Pennsylvania 15213

Dr. Ronald L. Huston
Dept. of Engineering Analysis
Mail Box 111
University of Cincinnati
Cincinnati, Ohio 45221

Prof. George Sih
Dept. of Mechanics
Lehigh University
Bethlehem, Pennsylvania 18015

Prof. A.S. Kobayashi
University of Washington
Dept. of Mechanical Engineering
Seattle, Washington 98105

Librarian
Webb Institute of Naval Architecture
Crescent Beach Road, Glen Cove
Long Island, New York 11542

Prof. Daniel Frederick
Virginia Polytechnic Institute
Dept. of Engineering Mechanics
Blacksburg, Virginia 24061

Prof. A.C. Eringen
Dept. of Aerospace & Mech. Sciences
Princeton University
Princeton, New Jersey 08540

Dr. S.L. Koh
School of Aero., Astro. & Engr. Sc.
Purdue University
Lafayette, Indiana 47907

Prof. E.H. Lee
Div. of Engrg. Mechanics
Stanford University
Stanford, California 94305

Prof. R.D. Mindlin
Dept. of Civil Engrg.
Columbia University
S.W. Mudd Building
New York, N.Y. 10027

Prof. S.B. Dong
University of California
Dept. of Mechanics
Los Angeles, California 90024
Prof. Burt Paul
University of Pennsylvania
Towne School of Civil & Mech. Engrg.
Rm. 113 - Towne Building
220 S. 33rd Street
Philadelphia, Pennsylvania 19104
Prof. H.W. Liu
Dept. of Chemical Engr. & Metal.
Syracuse University
Syracuse, N.Y. 13210

Prof. S. Bodner
Technion R&D Foundation
Haifa, Israel
Prof. R.J.H. Bolland
Chairman, Aeronautical Engr. Dept.
207 Guggenheim Hall
University of Washington
Seattle, Washington 98105

Prof. G.S. Heller
Division of Engineering
Brown University
Providence, Rhode Island 02912

Prof. Werner Goldsmith
Dept. of Mechanical Engineering
Div. of Applied Mechanics
University of California
Berkeley, California 94720

Prof. J.R. Rice
Division of Engineering
Brown University
Providence, Rhode Island 02912

Prof. R.S. Rivlin
Center for the Application of Mathematics
Lehigh University
Bethlehem, Pennsylvania 18015

Library (Code 0384)
U.S. Naval Postgraduate School
Monterey, California 93940

Dr. Francis Cozzarelli
Div. of Interdisciplinary
Studies & Research
School of Engineering
State University of New York
Buffalo, N.Y. 14214

Industry and Research Institutes

Library Services Department
Report Section Bldg. 14-14
Argonne National Laboratory
9700 S. Cass Avenue
Argonne, Illinois 60440

Dr. M. C. Junger
Cambridge Acoustical Associates
129 Mount Auburn St.
Cambridge, Massachusetts 02138

Dr. L.H. Chen
General Dynamics Corporation
Electric Boat Division
Groton, Connecticut 06340

Dr. J.E. Greenspon
J.G. Engineering Research Associates
3831 Menlo Drive
Baltimore, Maryland 21215

Dr. S. Batdorf
The Aerospace Corp.
P.O. Box 92957
Los Angeles, California 90009

Dr. K.C. Park
Lockheed Palo Alto Research Laboratory
Dept. 5233, Bldg. 205
3251 Hanover Street
Palo Alto, CA 94304

Library
Newport News Shipbuilding &
Dry Dock Company
Newport News, Virginia 23607

Dr. W.F. Bozich
McDonnell Douglas Corporation
5301 Bolsa Ave.
Huntington Beach, CA 92647

Dr. H.N. Abramson
Southwest Research Institute
Technical Vice President
Mechanical Sciences
P.O. Drawer 28510
San Antonio, Texas 78284

Dr. R.C. DeHart
Southwest Research Institute
Dept. of Structural Research
P.O. Drawer 28510
San Antonio, Texas 78284

Dr. M.L. Baron
Weidlinger Associates,
Consulting Engineers
110 East 59th Street
New York, N.Y. 10022

Dr. W.A. von Riesemann
Sandia Laboratories
Sandia Base
Albuquerque, New Mexico 87115

Dr. T.L. Geers
Lockheed Missiles & Space Co.
Palo Alto Research Laboratory
3251 Hanover Street
Palo Alto, California 94304

Dr. J.L. Tocher
Boeing Computer Services, Inc.
P.O. Box 24346
Seattle, Washington 98124

Mr. Willian Caywood
Code BBE, Applied Physics Laboratory
8621 Georgia Avenue
Silver Spring, Maryland 20034

Mr. P.C. Durup
Lockheed-California Company
Aeromechanics Dept., 74-43
Burbank, California 91503